SIGNIFICANCE OF SOFT VALLEY SEDIMENT IN ALTERING SPATIAL GROUND MOTIONS AND BRIDGE RELATIVE RESPONSE

Maher ADAM[1] and Nawawi CHOUW[2]

[1] Associate Professor, Civil Engineering Department (Shoubra), Zagazig University, Cairo, Egypt, maheradam@yalla.com
[2] Associate Professor, Faculty of Environmental Science and Technology, Okayama University, Okayama 700-8530, Japan, chouw@cc.okayama-u.ac.jp

The study addresses the influence of local soft valley sediment on incident wave propagation and the relative response of two adjacent bridge structures. In contrast to previous studies the effect of various angles and dominant frequencies of the incident waves and soil-structure interaction (SSI) is considered. The investigation reveals that the local soft soil can significantly alter the spatial variation and also frequency content of the surface ground motions. The simultaneous effect of soil-structure interaction and the spatially varying ground excitations due to inclined incident waves are significant for an adequate estimation of the damage potential of bridge girders due to poundings and insufficient seat length.

Key words: *Relative displacement, non-uniform ground motions, soil-structure interaction, bridge structure, local soft sediment*

1. INTRODUCTION

Bridge damages due to girder poundings or unseating have been observed in almost all major earthquake events such as the 1989 Loma Prieta earthquake[1)], the 1994 Northridge earthquake[2)] and the 1995 Kobe earthquake[3)]. Girder pounding and separation are strongly determined by the relative displacements of the adjacent girders. They are therefore defined not only by the ground motions but also the relationship between the dynamic properties of the adjacent bridge structures. Studies on bridge relative responses focused on the causes of pounding responses, how their damaging effect can be reduced, and on design recommendations for mitigating the earthquake load effect on the responses of adjacent structures. However, most of the studies are based on assumption of uniform ground excitation and fixed-based structures. DesRoches and Muthumar[4)], for example, investigated the response of two bridge segments using single-degree-of-freedom (sdof) systems. Ruangrassamee and Kawashima[5)] proposed relative displacement response spectra for determining girder seat length. Jankowski et al.[6)] investigated various measures for reducing pounding effects. Recommendation of many current design regulations such as by Caltrans[7)] or Japan Road Association[8)] are also based on these assumptions.

Since it is the nature of a bridge to span a large distance, such as a wide river or a valley, the bridge piers are often far apart. The ground motions at these distant pier locations are likely not the same owing to the propagation of seismic waves. Besides bridge structures on soft soil can behave differently than bridge on hard soil. Consequently, the results obtained from analyses with fixed-base structure assumption can differ from the ones with soil-structure interaction. Zanardo et al.[9)] and Chouw and Hao[10), 11)] confirmed the significance of the effect of spatially varying ground excitations on the relative bridge responses. Many works on pounding responses between bridge girders are published in the past, however, investigation on the simultaneous effect of inclined incident waves and local soft soil is unknown. In this study the effect of incident wave characteristics and the valley sediment on relative responses of two bridge segments is considered.

2. BRIDGE STRUCTURE, SUBSOIL AND INCIDENT WAVES

Figure 1 shows the considered system. Two subsoil configurations are chosen:

(1) A uniform half-space with a valley of 20 m depth and a width of 380 m at the bottom.

(2) The valley with soft sediment of 150 m depth (marked by dash-dotted line).

If soil-structure interaction is considered, a surface foundation of 9 m x 9 m is assumed. The bridge structures and their foundations are described by a finite element method, and the subsoil by a boundary element method. The displacements of the left and right girders are $u_1(t)$ and $u_2(t)$, respectively. When the approaching relative displacement $|u_1(t)-u_2(t)|$ is larger than the gap size, pounding takes place. When the separating relative displacement $|u_2(t)-u_1(t)|$ is larger than the seat length, unseating occurs. Corresponding to the current Japan Road Association design regulation[8] the relative responses are studied as a function of the fundamental frequency ratio of the adjacent bridge structures. It is assumed that the left and right bridge segments will experience only horizontal ground motions at the locations A and B (Figure 1). Both locations are 95 m away from the centerline of the valley. It should be mentioned that the simplification of a multiple-pier structure to a single-pier system might overestimated the spatial ground motion effect, because multiple-pier system tends to average out the influence of the spatial ground variation[12].

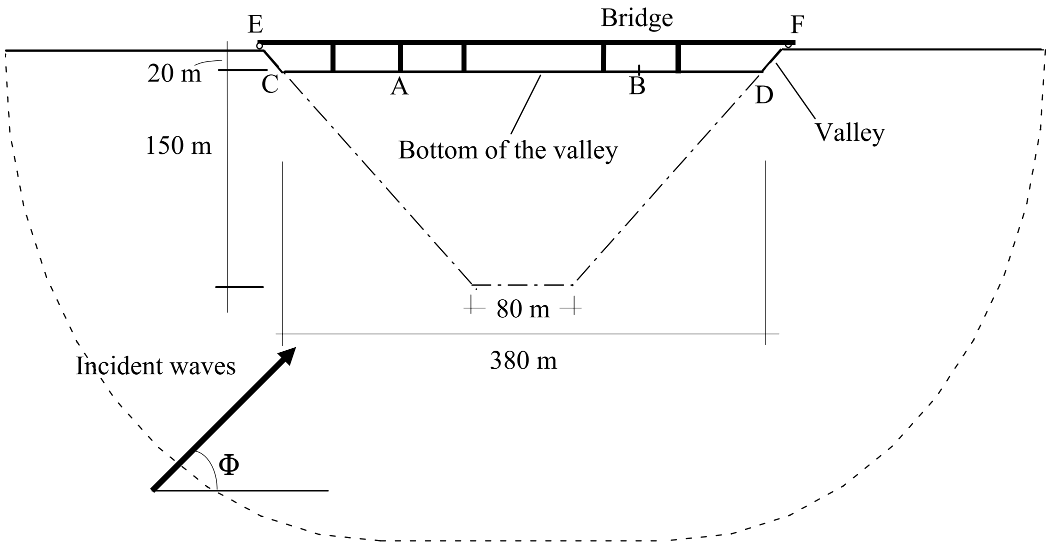

Figure 1. Overview of the considered system: bridge, valley and subsoil

The half-space consists of hard soil with a shear wave velocity of 600 m/s, a Poisson's ratio of 0.33 and a density of 2200 kg/m^3. The soft sediment has a shear wave velocity of 100 m/s, a Poisson's ratio of 0.33 and a density of 1800 kg/m^3. It is assumed that the subsoil has no material damping. In Figure 2 the two bridge segments are presented. For simplicity the displacement of each girder is described by a single-degree-of-freedom (sdof). Thus if the soil-structure interaction effect is neglected, each of the multiple-pier bridge segment is modeled as a sdof system with a mass of 1000 t (indicated in black) with an assumed fixed base.

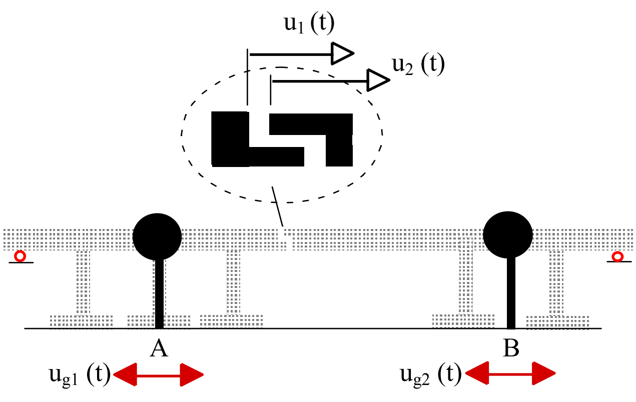

Figure 2. Simplified bridge model

In order to limit the influence factors and to enable a clear interpretation of the result, incident waves of a Ricker waveform with a single dominant frequency f_d is chosen. Figures 3(a) and (b) show respectively the time history ui and the corresponding Fourier spectrum amplitude |ui| of the wavelet with the dominant frequency f_d of 0.5 Hz. The direction of the wave propagation is defined by the angle Φ. The wave front is perpendicular to the wave propagation direction. In this study vertical wave propagation (Φ = 90°) and an inclined propagation with Φ = 30° are considered.

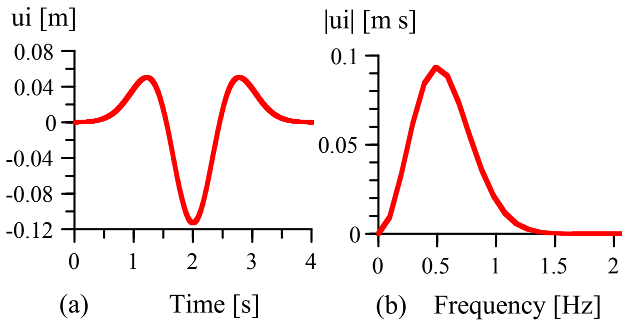

Figure 3. Incident ground displacement. (a) Time history ui(t) and its corresponding Fourier amplitude |ui| (f)

(1) Incident wave formulation

The differential equation of *Lamé-Navier* describes the displacement field of a linear-elastic continuum. Under the assumption of homogeneous initial conditions and vanishing body forces this differential equation can be transformed to the boundary integral equation[13)]

$$c_{ik}u_k(\xi,t)=\int_{\Gamma_\mathbf{x}}\int_0^t u^*_{ik}(\mathbf{x},t,\xi,\tau)t_i(\mathbf{x},\tau)\,d\tau\, d\Gamma_\mathbf{x} - \int_{\Gamma_\mathbf{x}}\int_0^t t^*_{ik}(\mathbf{x},t,\xi,\tau)u_i(\mathbf{x},\tau)\,d\tau\, d\Gamma_\mathbf{x} \tag{1}$$

where t^*_{ik} and u^*_{ik} are the fundamental solutions[14)] for traction and displacement at the field point $\mathbf{x}$ at time t, caused by a *Dirac*-load acting at the boundary point ξ at time τ. u_i and t_i represent displacement and the traction boundary values. $\Gamma_\mathbf{x}$ is the integration over the boundary Γ with respect to $\mathbf{x}$. The matrix c_{ik} includes the integral-free terms, which depend on the geometry in the vicinity of the source point ξ.

For the case of scattering of incident waves Equation (1) cannot be applied directly to the total wave field, because it does not satisfy the radiation conditions. The superposition of the incident and scattered wave fields is thus applied and Equation (1) takes the form

$$c_{ik}u_k(\xi,t)=\int_{\Gamma_\mathbf{x}}\int_0^t u^*_{ik}(\mathbf{x},t,\xi,\tau)t_i(\mathbf{x},\tau)\,d\tau\, d\Gamma_\mathbf{x} - \int_{\Gamma_\mathbf{x}}\int_0^t t^*_{ik}(\mathbf{x},t,\xi,\tau)u_i(\mathbf{x},\tau)\,d\tau\, d\Gamma_\mathbf{x} + ui_i(\mathbf{x},t) \tag{2}$$

where ui_i is the incident displacement vector at the boundary. Generally, for each point on the boundary Γ either the displacement or the traction are known, and Equation (2) is used to determine the unknown boundary values.

For the numerical solution, the boundary integral equation (2) is discretized in time and space and then solved. The time integration of Equation (2) for the boundary values can be carried out analytically leading to functions that depend on space variables only. For arbitrary boundary geometry, these functions cannot be integrated analytically. Therefore, the boundary Γ is divided into constant, linear or quadratic isoparametric boundary elements. Equation (2) can be written in the form

$$c_{ik}u_i(\xi,t_N)+\sum_{l=1}^{L}\sum_{m=1}^{N}\int_{\Gamma_l} T_{ik}^{(N-m+1)}(\mathbf{x},\xi)\,d\Gamma_{l\mathbf{x}}\,{}^{(l)}u_i^{(m)} - {}^{(l)}ui_i^{(m)} = \sum_{l=1}^{L}\sum_{m=1}^{N}\int_{\Gamma_l} U_{ik}^{(N-m+1)}(\mathbf{x},\xi)\,d\Gamma_{l\mathbf{x}}\,{}^{(l)}t_i^{(m)} \tag{3}$$

where T_{ik} and U_{ik} are the traction and displacement kernels, respectively, resulting from the temporal integration of the fundamental solution. The outer summation in Equation (3) is carried out over the total number of elements L and the inner one is carried out over the number of time steps N. After integration, Equation (3) can be written in matrix notation as:

$$\begin{aligned}\mathbf{U}^1\mathbf{t}^N &= \mathbf{T}^1\mathbf{u}^N + \mathbf{E}^N - \mathbf{ui}^N,\\ \mathbf{E}^N &= \sum_{m=2}^{N}\mathbf{T}^m\mathbf{u}^{N-m+1} - \mathbf{U}^m\mathbf{t}^{N-m+1}\end{aligned} \tag{4}$$

where $\mathbf{U}^m$ and $\mathbf{T}^m$ are the coefficient matrices of the system at time $m\,\Delta t$. For the current time step N, all traction vectors $\mathbf{t}^m$, m = 1 to N, and previous displacement vectors $\mathbf{u}^m$, m = 1 to N-1, are known. More details and verification of the algorithm can be found in Adam et al.[15)]. The validity of the approach has been verified in a comparison of the results with the ones obtained using 3D BEM approach in the time domain[15)].

(2) Relative response of adjacent bridge structures

In the analysis of girder relative responses the bridge structures with foundations and the subsoil are described in the Laplace domain using finite elements and boundary elements, respectively. To incorporate the effect of girder pounding and separation the analysis is performed subsequently in the Laplace and time domain. The governing equation of each bridge segment with subsoil in the Laplace domain is

$$\begin{bmatrix}\tilde{\mathbf{K}}^{\mathrm{bn}}_{\mathrm{bb}} & \tilde{\mathbf{K}}^{\mathrm{bn}}_{\mathrm{bc}}\\ \tilde{\mathbf{K}}^{\mathrm{bn}}_{\mathrm{cb}} & \tilde{\mathbf{K}}^{\mathrm{bn}}_{\mathrm{cc}}+\tilde{\mathbf{K}}^{\mathrm{sn}}_{\mathrm{cc}}\end{bmatrix}\begin{Bmatrix}\tilde{\mathbf{u}}^{\mathrm{bn}}_{\mathrm{b}}\\ \tilde{\mathbf{u}}^{\mathrm{bn}}_{\mathrm{c}}\end{Bmatrix}=\begin{Bmatrix}\tilde{\mathbf{P}}^{\mathrm{bn}}_{\mathrm{b}}\\ \tilde{\mathbf{P}}^{\mathrm{bn}}_{\mathrm{c}}\end{Bmatrix} \tag{5}$$

The superscripts b and s stand for the bridge and subsoil, respectively. The superscript n indicates the left or the right bridge segment. The subscripts b and c stand for bridge and contact-degree-of-freedom at the interface between the bridge pier foundation and the subsoil, respectively. The tilde indicates a vector or matrix in the Laplace domain.

After transforming the surface ground motions from the time domain into the Laplace domain

$$\{\tilde{\boldsymbol{P}}(s)\} = \int_0^\infty \{\boldsymbol{P}(t)\} e^{-st} dt \qquad (6)$$

where $s = \delta + i\omega$ is the Laplace parameter and $i = \sqrt{-1}$, the linear response $\{\tilde{\boldsymbol{u}}(s)\}$ of both bridge structures can be obtained using Equation (5). A transformation of the results from the Laplace to the time domain gives the time history of the structural responses, and the girder relative displacements can be determined.

$$\{\boldsymbol{u}(t)\} = \frac{1}{2\pi i} \int_{\delta - i\omega}^{\delta + i\omega} \{\tilde{\boldsymbol{u}}(s)\} e^{st} ds \qquad (7)$$

By examining the linear relative responses the instant when pounding takes place can be determined. To incorporate the pounding effect the unbalanced forces are defined using the relative displacement and the condensed stiffness of one of the subsystems

$$\tilde{\mathbf{K}}^{n*}_{pp} = \tilde{\mathbf{K}}^{n}_{pp} - (\tilde{\mathbf{K}}^{n}_{pu} (\tilde{\mathbf{K}}^{n}_{uu})^{-1} \tilde{\mathbf{K}}^{n}_{up}) \qquad (8)$$

The subscripts p and u stand for the pounding-degree-of-freedom and the other dofs of the considered subsystem. Since the two subsystems are now in contact the condensed stiffness has to be added to the stiffness of the uncondensed subsystem. Using the unbalanced forces and the stiffness of the coupled subsystems the corrective term can be determined, and the linear responses are corrected in the time domain from the instant when the pounding occurs. An examination of the results reveals the instant when the girders separate, e.g. at time t_s. The unbalanced force to incorporate the separation effect is equal to the contact force. The corrective term is determined using Equation (5) of the uncoupled subsystems. Using the corrective term the results can be corrected from time t_s. The actual responses are checked again for further poundings. The calculation is complete if no more pounding or separation occur. Details of the nonlinear soil-structure interaction procedure are described in the reference[16]. The validity of the approach has been confirmed in a comparison of the results with those obtained directly in the time domain using a step-by-step numerical integration procedure[16].

3. ALTERATION OF GROUND MOTIONS

Figures 4(a) and (b) show the alteration of the maximum ground surface displacement and acceleration due to the hard soil valley, respectively. The ratios $u_{g,\,max}$ / $u_{i,\,max}$ (-) and $a_{g,\,max}$ / $a_{i,\,max}$ (-) are the amplification factors of the surface ground motions with respect to the maximum incident ground displacement $u_{i,\,max}$ and its corresponding ground acceleration $a_{i,\,max}$. If the valley does not exist, the displacements and accelerations at all surface locations will experience an amplification factor of 2.0. The 20 m depth valley reduces the ground motions around the edges (locations C and D in Figure 1). Amplification takes place at about the middle of the valley escarpments (between C and E, and D and F). While incident waves with f_d of 0.5 Hz causes a reduction along the valley bottom, all other incident waves with higher frequencies produce almost the same ground displacement at the valley centerline as the case without a valley. Incident waves with f_d of 1.0 Hz even amplify the ground acceleration (Figure 4(b)). The alteration of the peak ground displacement (PGD) and acceleration (PGA) depends strongly on the frequency content of incident waves and the shape of the valley.

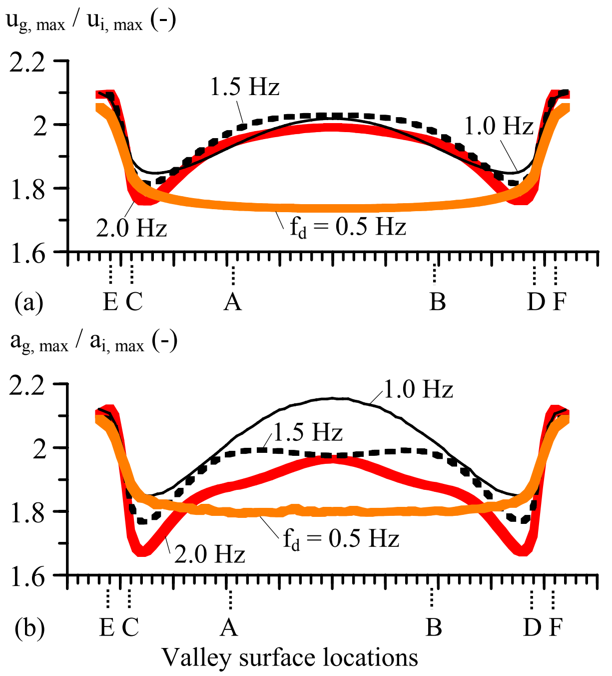

Figure 4(a) and (b). Alteration of horizontal ground motions along the valley surface. (a) Maximum surface displacements and (b) surface accelerations

In Figure 5 the influence of the incident wave dominant frequency f_d, and incident angle Φ on the ground displacements and accelerations at the locations A and B is displayed. The left, middle and right columns show the ground motions due to

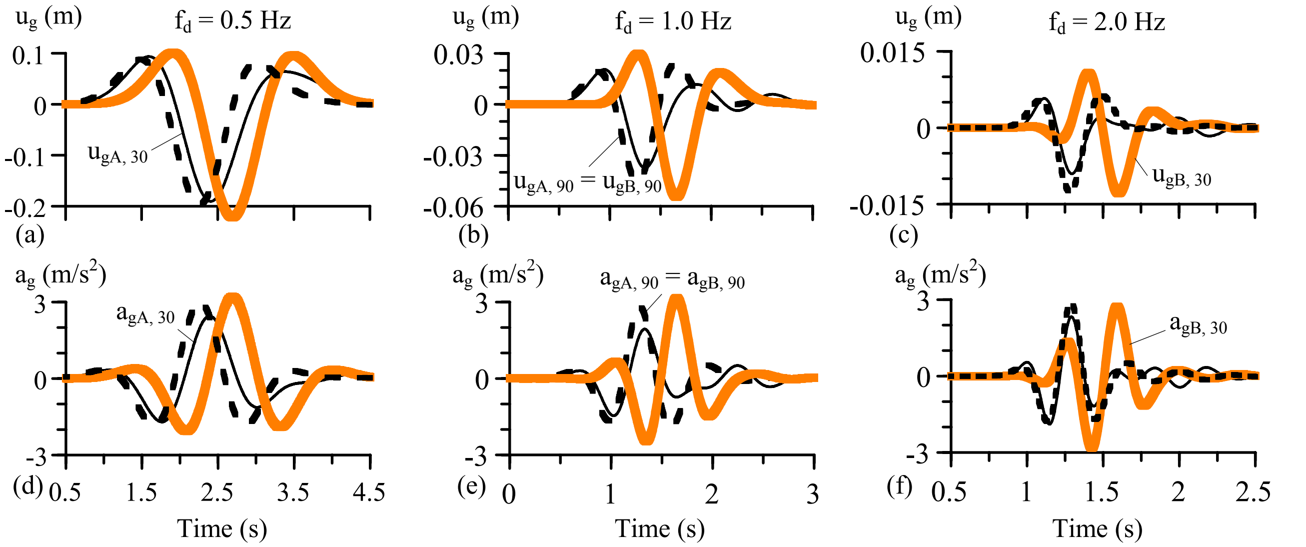

Figure 5(a)-(f). Effect of the dominant frequency f_d and propagation angle of the incident waves on the non-uniform half-space ground motions. (a)-(b) Ground displacements u_g and (d)-(f) ground accelerations a_g

incident waves with f_d of 0.5 Hz, 1.0 Hz and 2.0 Hz, respectively. In Figure 6 an additional effect of soft sediment is considered. Since the valley has a symmetrical shape, vertically propagating waves will produce the same ground motions. The inclined incident waves cause clearly non-uniform ground motions, and the amplitude at the left pier location A is smaller than the one at the right pier location B. In the case of uniform hard soil the influence of the wave dominant frequency f_d can be seen in the change of the ground displacement amplitudes. Even though all cases have almost the same PGA around 3 m/s^2, incident waves with low dominant frequencies cause larger surface ground displacements (compared, e.g. Figure 5(c) with 5(a)). In the case of valley with local soft soil lower dominant frequencies of incident waves cause larger ground displacements (Figures 6(a)-(c)), and also accelerations (Figures 6(d)-(f)). Compared with the case of uniform hard soil the local soft sediment generates longer duration of ground motions. The inclined incident waves with f_d of 1.0 Hz and 0.5 Hz produce much stronger ground motions (thin and bold lines) than the one due to vertically propagating incident waves (bold dotted line).

Figure 7 shows the alteration of the frequency content of surface ground accelerations along the valley due to the local soft sediment. The left and right columns are the case without and with local sediment, respectively. Only vertically propagating incident waves are considered. The dominant frequency increases with the incident wave frequencies f_d of 0.5 Hz, 1.0 Hz, 1.5 Hz and 2.0 Hz correspondingly from 0.85 Hz, 1.65 Hz, 2.4 Hz to 3.2 Hz.

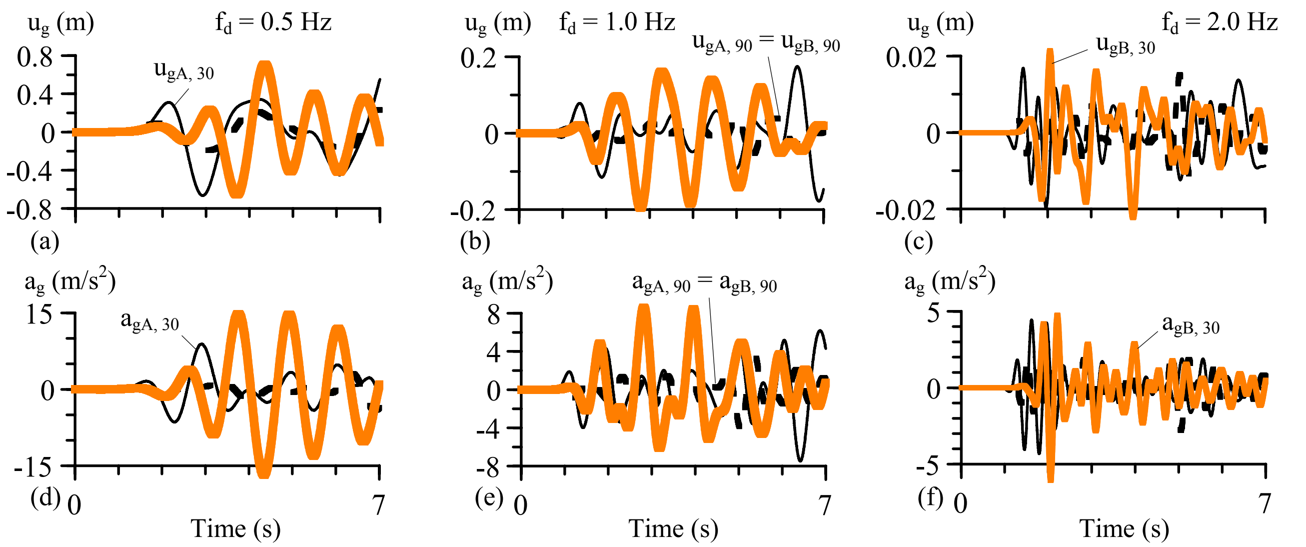

Figure 6(a)-(f). Effect of the dominant frequency f_d, propagation angle of the incident waves and local soft soil sediment on the non- uniform half-space ground motions. (a)-(b) Ground displacements u_g and (d)-(f) ground accelerations a_g

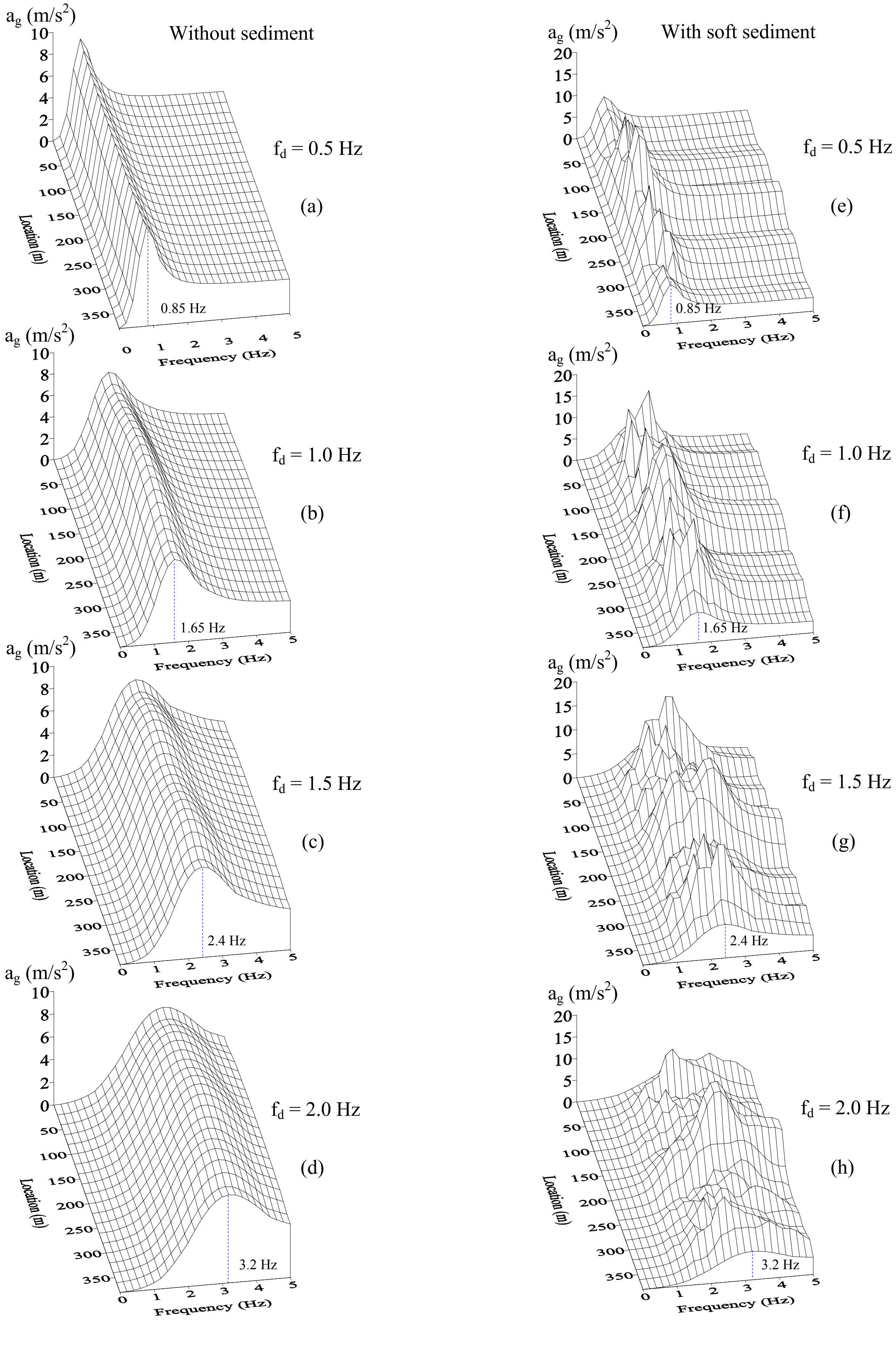

Figure 7(a)-(d). Influence of the dominant frequency f_d of the incident waves on the response spectra of surface ground acceleration along the valley bottom with a damping ratio of 5 %. (a)-(d) Uniform hard soil and (e)-(h) soft sediment over hard soil

Figure 8 shows the maximum response spectrum values of the surface ground accelerations along the valley without local soft sediment. With increasing f_d the values alter strongly along the valley.

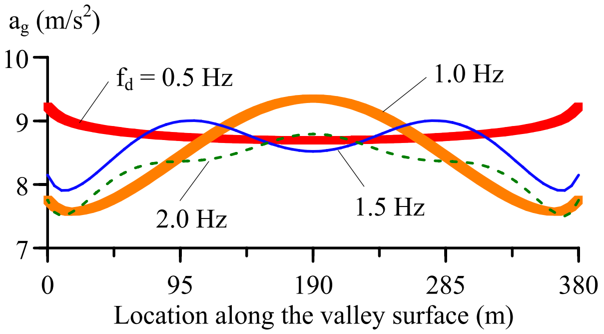

Figure 8. Influence of the dominant frequency f_d of the incident waves on the alteration of the ground motion frequency content along the hard soil valley bottom surface

In Figure 9 the additional effect of the local soft soil is presented. The results clearly show that compared to the valley effect the local soft sediment causes much stronger alteration of the frequency content of the ground motions along the valley.

4. RELATIVE RESPONSE OF ADJACENT BRIDGE STRUCTURES

In this study it is assumed that the gap between the girders is 0.05 m, and the fundamental frequency f_l of the left bridge segment with an assumed fixed base is always 1.0 Hz.

Figure 10 shows the SSI effect on girder displacements. Uniform ground excitations and a fundamental frequency ratio f_2/f_l of 1.0 are assumed. The bridge is located on the soft sediment, and the incident waves with the propagation angle Φ of 30° have the dominant frequency f_d of 2.0 Hz. The displacements u_l and u_2 of the left and right girders without SSI are plotted as dash and dash-dotted lines, respectively, and the ones with SSI as thin and bold lines. The result without SSI confirms the recommendation of many current design regulations such as Caltrans[7)] or Japan Road Association[8)] for mitigating pounding by adjusting the natural frequencies of neighbouring structures. If the considered adjacent structure have the same fundamental frequency and experience the same ground motions, thus both girders respond in phase. Consequently, no pounding takes place. If SSI is considered, smaller girder responses can be observed, because in the considered case the soft subsoil move the system fundamental frequency further away from the dominant frequency of the ground motions. Pounding also does not occur.

If non-uniform ground accelerations are considered,

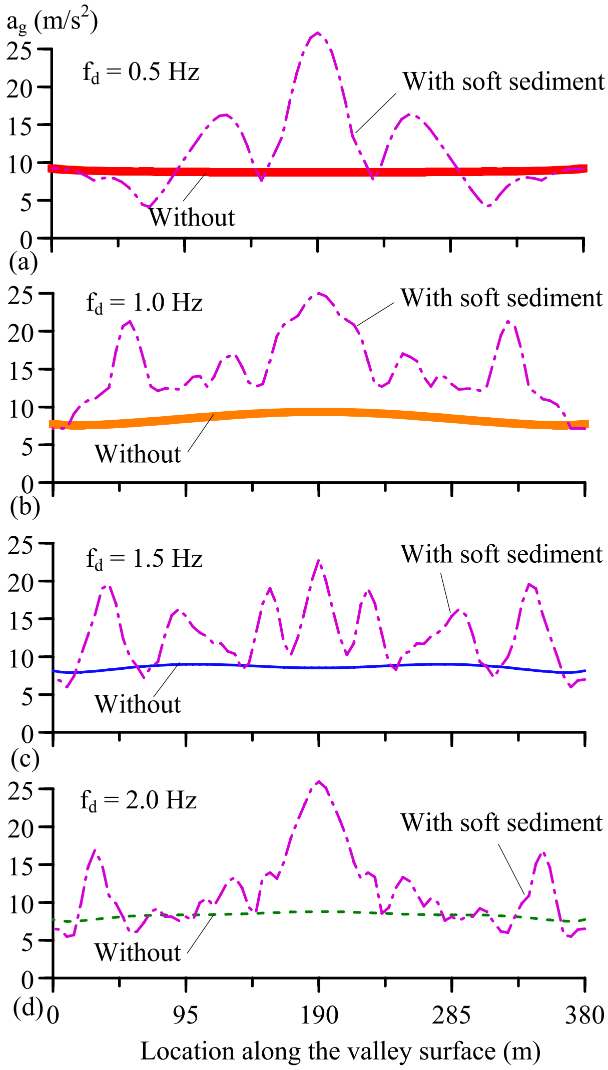

Figure 9(a)-(d). Effect of the soft soil sediment on the alteration of the frequency content of the ground acceleration along the valley bottom due to incident waves with the dominant frequency fd of (a) 0.5 Hz, (b) 1 Hz, (c) 1.5 Hz and (d) 2 Hz

a fixed base assumption of the bridge structures will also cause no pounding (u_l = dash line, and u_2 = dash-dotted line in Figure 11). SSI will, however, cause pounding, e.g. at 5.8 s, 7.0 s or 8.1 s (u_l = thin line, and u_2 = bold line).

Figure 12 shows the girder responses with and without poundings due to non-uniform ground motions including the quasi-static responses owing to spatially varying ground displacements. Even though the ground displacements with a maximum value of around 0.02 m (see Figure 6(c)) are not large compared to the one due to incident waves with f_d of 0.5 Hz (Figure 6(a)), they cause a later first pounding at 7.0 s (compared to the response at 5.8 s in Figures 11 and 12). In the considered case both considered bridge segments are equally strong. However, the right bridge segment experiences stronger excitation. Consequently, it can force its way, and causes a reduction of the left girder response.

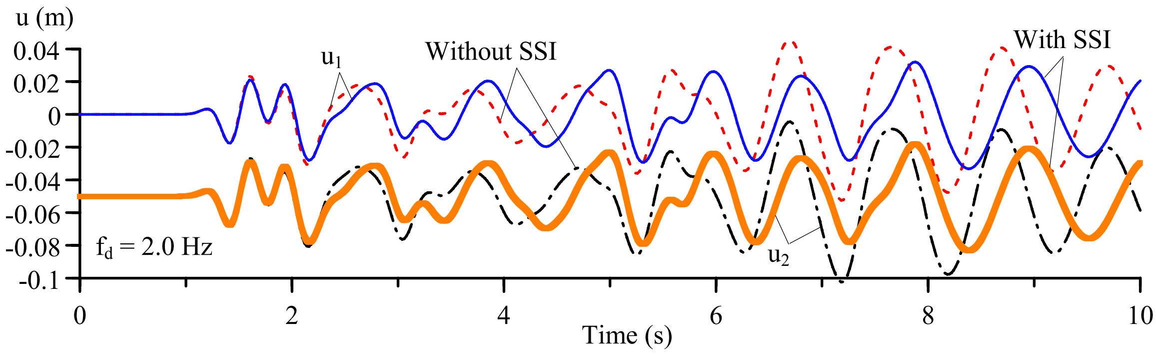

Figure 10. Effect of soil-structure interaction on uniform ground motion induced structural responses u_1 and u_2. f_d = 2.0 Hz

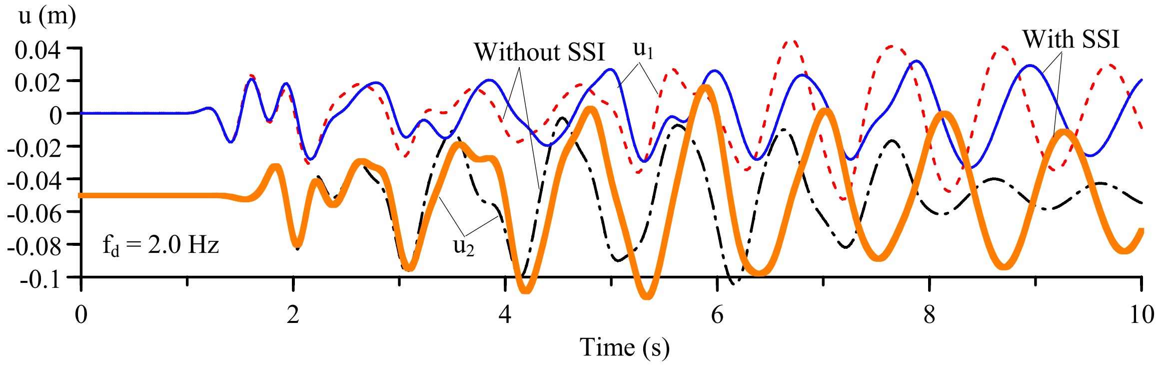

Figure 11. Effect of soil-structure interaction and non-uniform ground excitation with f_d = 2.0 Hz on linear girder responses u_1 and u_2

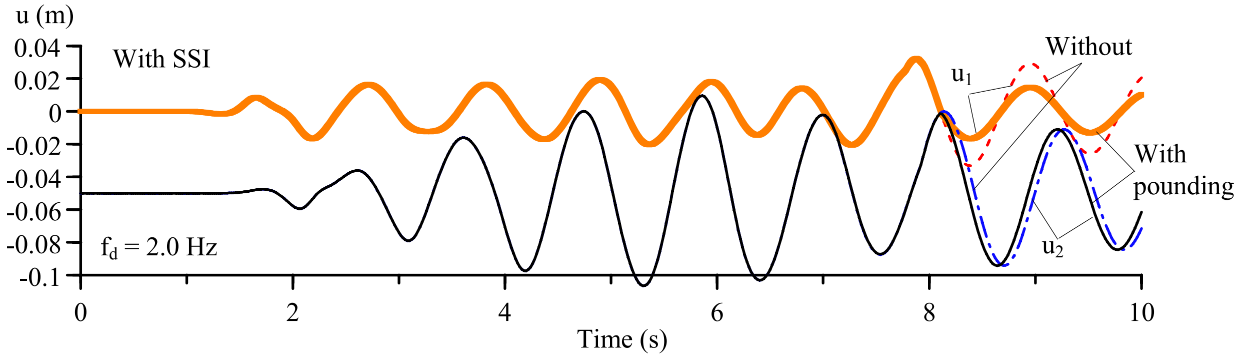

Figure 12. Effect of soil-structure interaction, quasi-static response, non-uniform ground excitation with f_d = 2.0 Hz and pounding on girder responses u_1 and u_2

The results clearly show that the commonly followed approach by assuming uniform ground excitations can underestimate the pounding potential, and consequently the damages of structures.

Figure 13 shows the effect of non-uniform ground excitations, the dominant frequency of incident waves and their propagation direction on the girder relative displacements. The effect of the local soft soil is not considered. Since the uniform soil is hard, SSI effect is neglected. The responses are given as a function of the fundamental frequency ratio f_2/f_1 of the right bridge segment to the left structure. The approaching and separating displacements are the displacements when the two girders come closer toward each other and when they move away from each other, respectively. They are indicated by solid, dash or dash-dotted lines correspondingly. Except the results in Figure 15 caused by vertically propagating waves, all results are due to incident waves with $\Phi$of 30°.

In Figure 13(a) uniform ground excitations (a_{g2} = a_{g1}) and fixed-base structures are assumed as performed in most of current practices. In the case of a frequency ratio f_2/f_1 of 1.0 the in-phase responses will not cause pounding or separation. The approaching displacement with pounding effect of 0.05 m represents the chosen gap size (dash-dotted line). If the right structure is stiff, poundings cause a reduction of the required seat length (black solid line). In contrast, if the right bridge segment is more flexible than the left bridge structure, poundings cause an amplification of the required seat length (compared solid thin with solid bold line for f_2/f_1 below 0.5).

If actual non-uniform ground excitations a_{g1} and a_{g2} are considered, the relative responses can be totally different (Figure 13(b)). The most significant difference can be seen just when the frequency ratio f_2/f_1 is 1.0. The relative displacement is no longer zero. The reason is that the inclined incident waves cause non-uniform ground motions at the valley surface, even though both bridge piers are located symmetrically with respect to the centerline of the valley. While both bridge structures will respond to an assumed uniform ground excitation in phase owing to their same fundamental frequency, the bridge segments will respond to the strongly non-uniform ground excitation just out of phase. The recommendation of many current design regulations to adjust the fundamental frequency of the structure with the one of the adjacent structure can lead to just an opposite effect, when it can be ensured that the ground motions are spatially varied.

If the quasi-static responses owing to spatially varying ground displacements at the two bridge pier locations are considered as well (Figure 13(c)), in the higher frequency-ratio range poundings do not reduce the separating relative displacement much. The separating displacements are clearly determined by the quasi-static responses. In the lower frequency-ratio range the quasi-static responses have only minor influence. The results show that a neglect of non-uniform ground displacements in the analysis can clearly underestimate the required seat length to avoid bridge girders from unseating.

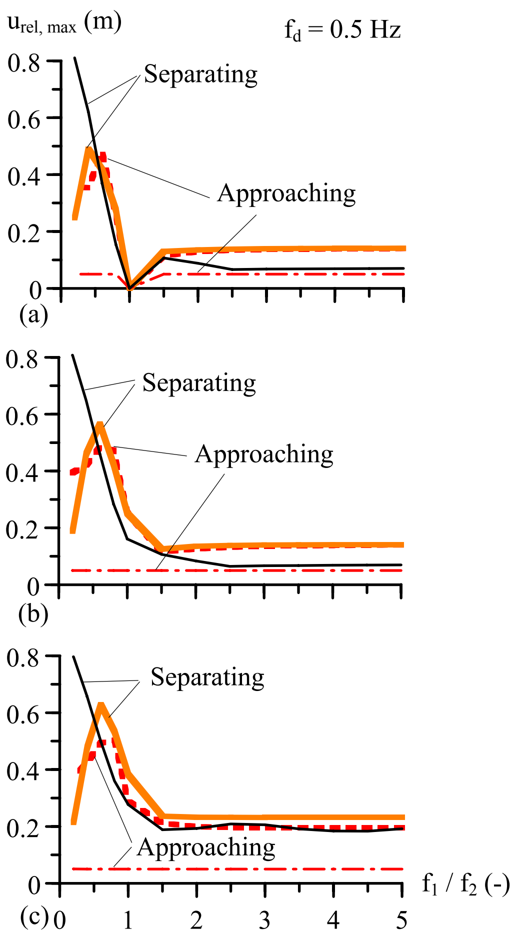

Figure 13(a)-(c). Relative displacement due to incident waves with the dominant frequency f_d of 0.5 Hz. (a) Uniform ground excitation, (b) non-uniform ground excitation, and (c) non-uniform ground excitation with quasi-static responses

Figures 14(a) and (b) show the relative displacements due to incident waves with the dominant frequencies f_d of 1.0 Hz and 2.0 Hz, respectively. Compared to those due to incident waves with f_d of 0.5 Hz, the responses are much smaller. In the case f_d of 2.0 Hz they are so small that poundings do not take place at all (Figure 14(b)). Even though all incident waves with f_d of 0.5 Hz, 1.0 Hz and 2.0 Hz produce surface ground accelerations with similar PGA around 3 m/s^2, the resulting relative displacements are different. The results show that PGA alone is not sufficient for estimating the pounding potential of bridge girders, the dominant frequency of the ground motions is also significant. Low-frequency incident waves can cause large spatially varying ground displacements. Since the relative displacement is not only determined by the ground accelerations but also by the quasi-static response, the large non-uniform ground displacements can therefore significantly increase the relative displacement responses, and consequently increase the pounding as well as unseating potential of bridge girders.

Figure 15 shows the relative displacements due to vertically propagating incident waves with f_d of 0.5Hz. Since in this case the ground motions at the two bridge pier locations are the same, the ground displacements have no contribution to the relative displacement even though they are relatively large (dash line in Figure 5(a)). The result is similar to the one obtained with an assumption of uniform ground excitations in Figure 13(a). A comparison with the responses in Figure 13(c) clearly shows the influence of the propagation angle of the incident waves.

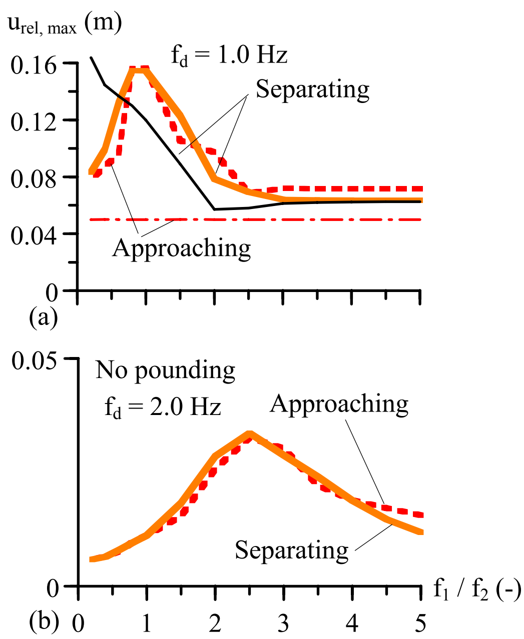

Figure 14(a) and (b). Relative displacement including quasi-static responses due to non-uniform ground excitation with the dominant frequency f_d of (a) 1.0 Hz and (b) 2.0 Hz

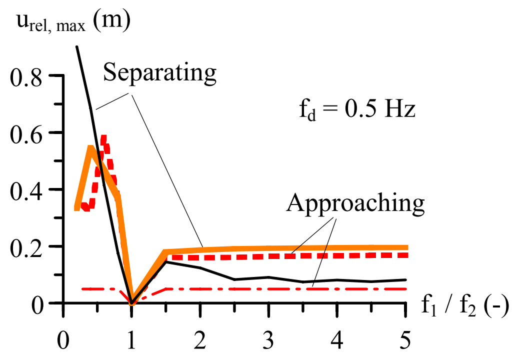

Figure 15. Relative displacement due to vertically propagating incident waves with f_d of 0.5 Hz

5. CONCLUSIONS

The effect of incident wave characteristics, soft local soil sediment of a trapezoidal shape valley, soil-structure interaction and bridge girder pounding on the relative response of two adjacent bridge structures is presented. The structures are described using finite elements and the subsoil using boundary elements. The local soil consists of 150 m depth soft valley sediment. The incident waves have an angle of 30^o and 90^o with the dominant frequencies of 0.5 Hz, 1.0 Hz, 1.5 Hz and 2.0 Hz. The following results are therefore only valid for the considered cases.
The investigation reveals:

Uniform hard soil valley (without local soft soil) reduces the PGA around the valley edges. Although all incident waves produce almost the same PGA, the PGD becomes larger with decreasing dominant frequency of the incident waves.

Soft sediment amplifies ground accelerations and also ground displacement at the valley surface.

Inclined incident waves generate strong spatial variation of ground motions, even at the bridge pier locations symmetrically located with respect to the valley centerline. The large non-uniform ground displacements cause large quasi-static responses, and consequently increase the relative responses, especially of stiff bridge structures.

If bridge structures are flexible, pounding can amplify the unseating potential of their girders.

Depending on the relationship between structural frequencies and the dominant frequencies of incident waves, SSI can have beneficial and adverse effect.

ACKNOWLEDGMENT: The authors wish to thank the Japanese Association of International Education for supporting the first author research stay at Okayama University. Thanks are also due to the Japanese Ministry of Education, Science, Sports and Culture for the support (award number 15560404) and the anonymous reviewers for their helpful comments.

REFERENCES

1) Yashinsky, M., Karshenas, M. J.: *Fundamental of seismic protection for bridges*, Earthquake Engineering Research Institute, 184pp., 2003.
2) Mohle, J., Fenves, G., Mayes, R., Priestley, N., Seible, F., Uang, C.-M., Werner, S., Aschheim, M.: Highway bridges and traffic management, *Earthquake Spectra*, **11(S2)**, 287-372, 1995.
3) Park, R., Billings, I. J., Clifton, G. C., Cousings, J., Filiatrault, A., Jennings, D. N., Jones, L. C. P., Perrin, N. D., Rooney, S. L., Sinclair, J., Spurr, D. D., Tanaka, H., Walker, G.: The Hyogo-ken Nanbu earthquake of 17 January 1995, Report of the NZNSEE Reconnaissance team, *Bulletin of the New Zealand National Society for Earthquake Engineering*, **28(1)**, 98 pp., 1995.
4) DesRoches, R., Muthukumar, S.: Effect of pounding and restrainers on seismic response of multiple-frame bridges, *J. of Structural Engineering*, ASCE, **128(7)**, 860-869, 2002.
5) Ruangrassamee, A., Kawashima, K.: Relative displacement response spectra with pounding effects, *Earthquake Engineering and Structural Dynamics*, **30**, 1511-1538.
6) Jankowski, R., Wilde, K., Fujino, Y.: Reduction of pounding effects in elevated bridges during earthquakes, *Earthquake Engineering and Structural Dynamics*, **29**, 195-212, 2000.
7) Caltrans Seismic Design Criteria: *Design manual-version 1.1*. California Dept. of Transportation, Sacramento, 1999.
8) Japan Road Association: *Specifications for highway bridges –Part V seismic design*, Fifth edition, 2004. (in Japanese)
9) Zanardo, G., Hao, H., Modena, C.: Seismic response of multi-span simply supported bridges to a spatially varying earthquake ground motion, *Earthquake Engineering and Structural Dynamics*, **31**, 1325-1345, 2002.
10) Chouw, N., Hao, H.: Effect of simultaneous spatial near-source ground excitation and soil on the pounding response of bridge girders, *J. of Applied Mechanics*, JSCE, **6**, 779-788, 2003.
11) Chouw, N., Hao, H.: Influence of SSI and frequency content of non-uniform ground motions on bridge girder poundings, *J. of Applied Mechanics*, JSCE, **7**, 841-851, 2004.
12) Hao, H.: Torsional response of building structure to spatial random ground excitations, *Engineering Structures*, **19**, 105-112, 1997.
13) Dominguez J. *Boundary Elements in Dynamics*. Computational Mechanics Publications Southampton/Boston: Elsevier Applied Science, London/New York, 1993.
14) Stokes G. G. On the dynamical theory of diffraction. *Transactions of Cambridge Philosophical Society*, **9**, 793-797, 1849.
15) Adam, M, Pflanz, G., Schmid, G. Two- and three-dimensional modelling of half-space and train track embankment under dynamic loading. *Soil Dynamics and Earthquake Engineering*, **19(8)**, 559-573, 2000.
16) Chouw, N.: Influence of soil-structure interaction on pounding response of adjacent buildings due to near-source earthquakes, *J. of Applied Mechanics*, JSCE, **5**, 543-553, 2002.

(Received March 14, 2005)